

Electronic Supplementary Information

The effects of plasma treatment on bacterial biofilm formation on vertically aligned carbon nanotube arrays

Samuel Yick,^{ab} Anne Mai-Prochnow,^a Igor Levchenko,^{ab} Jinghua Fang,^{ac} Michelle K. Bull,^d

Mark Bradbury,^d Tony Murphy^a and Kostya (Ken) Ostrikov^{abe}

^a Plasma Nanoscience Laboratories, Manufacturing Flagship, Commonwealth Scientific and Industrial Research Organisation (CSIRO), P.O. Box 218, Lindfield, NSW 2070, Australia.

^b Complex Systems, School of Physics, The University of Sydney, Sydney, NSW 2006, Australia.

^c School of Physics, University of Melbourne, Parkville, VIC 3010, Australia.

^d Processing Microbiology, Food and Nutrition Flagship, CSIRO, P.O. Box 52, North Ryde, NSW 1670, Australia.

^e School of Chemistry, Physics, and Mechanical Engineering, Queensland University of Technology, Brisbane, QLD 4000, Australia.

Contents:

S1. Schematic of the experimental setup

S2. Schematic of the ICP plasma setup

S3. Details of the SEM characterization

S4. Details of the Raman characterization

S5. Details of the XPS characterization

S6. Flow cytometry

S7. The effects plasma treatment on CNT arrays have on *S. epidermidis* and *P. aeruginosa*

S1. Schematic of the furnace-based experimental setup

The carbon nanotube samples were grown in a quartz tube of a thermal furnace (MTI, OTF-1200). The furnace includes vacuum pump, gas supply system, and gas flow regulator (Fig. S1).

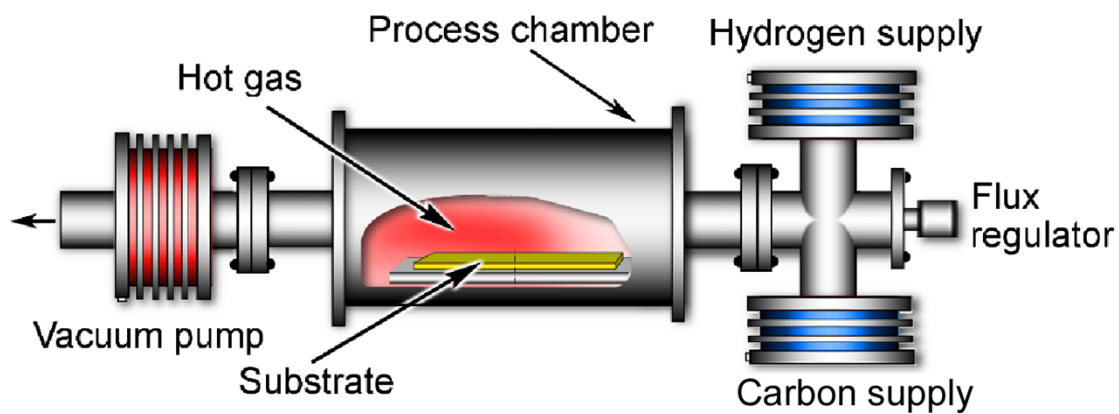


Fig. S1. Schematic of the furnace-based experimental setup used for growing CNT arrays

S2. Schematic of the ICP plasma setup

An inductively coupled plasma-enhanced chemical vapour deposition (ICP-CVD, with the operational frequency of 13.56 MHz and discharge power of about 1.0 kW) setup was used for the post-treatment of the carbon nanotube arrays. The plasma was ignited in a 5 Pa of Ar.

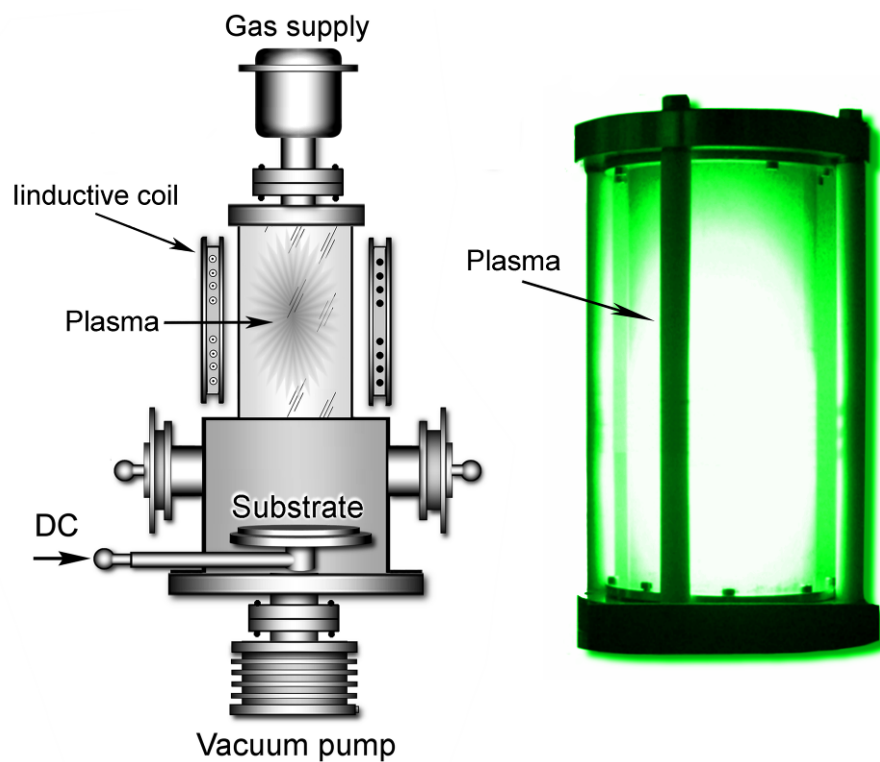


Fig. S2. Schematic of the ICP experimental setup used for treatment of the nanotube arrays

S3. Details of the SEM characterization

The morphology of the CNT arrays was examined using a field-emission scanning electron microscope (SEM). In order to utilise electron microscopic analysis, the bacteria laden samples were prepared with the critical point drying (CPD). The samples were first immersed in 100% ethanol, then transferred to the CPD chamber (BAL-TEC CPD030 Critical Point Dryer) and dried using liquid CO₂ for 3 hours at the critical point (+31.1°C, 1000 PSI). This process allows the structural integrity of both the bacteria and CNT arrays to be preserved in a high vacuum environment.

S4. Details of the Raman characterization

The spectra plotted in Figure S3 displayed features commonly associated with multi-walled CNTs. These features included the defect-induced mode (D-peak) at 1340 cm^{-1} , the graphitic mode (G-peak) at 1570 cm^{-1} and second-order feature (2D-peak) at 2680 cm^{-1} . Despite their similarity, the differences between the two spectra, namely the change in the relative intensity of the D and G-peak, the reduction of the 2D-peak and the emergence of a shoulder feature at 1604 cm^{-1} are apparent. The ratio between the D and G-peaks (I_D/I_G) reflects the crystalline order of the nanostructure. After plasma treatment, the I_D/I_G ratios of the respective samples increased from 0.65 to 1.26, thus implying a greater quantity of sp^3 carbon compared to the existing sp^2 graphitic structure. The increase in I_D/I_G ratio was accompanied by the reduction of the 2D peak. Such changes mean that the plasma treatment caused a disruption to the graphitic structure of the CNTs. The plasma treatment also resulted in the emergence of a shoulder feature (the D' peak) at 1604 cm^{-1} , which is due to the defect-induced single-phonon intravalley scattering process (from perturbations within the sp^2 lattice induced by the presences of voids and edge defects). Therefore, the D' peak in the plasma-treated sample can be attributed to the introduction of vacancies to the graphitic structure and the opening of the tubes. Thus, the information obtained from Raman analysis indicated that the plasma treatment created reactive sites without significantly affecting the morphology and overall graphitic nature of the whole CNT array. The presences of these reactive sites allow oxygen in the atmosphere to functionalize the CNT arrays.

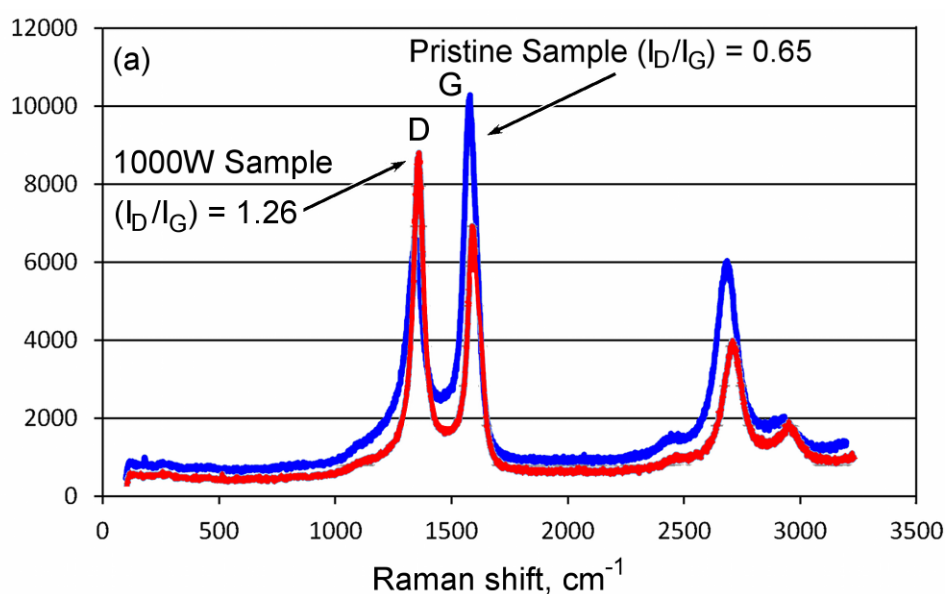


Fig. S3. Raman spectra

S5. Details of the XPS characterization

The chemical composition of the array was quantified by XPS. From the survey scans of the two samples (Figure S1), only carbon atoms were detected in the pristine sample; whereas oxygen atoms were also present in the 1000W plasma treated sample. **Figure S4** presents high-resolution scans over the regions of 280-295 eV and 524-542 eV, which correspond to the binding energy of the C1s and O1s feature respectively. These peaks were deconvoluted to reveal the different chemical environment exhibited by the pristine and the plasma treated CNT arrays. Within the pristine sample, three peaks at positions 284.52, 285.27 and 290.71 eV can be fitted under the C1s feature; these peaks corresponds to carbon in sp^2 - bonding, sp^3 - bonding and shake-up features generated from sp^3 carbon respectively (Figure 4a). After the plasma treatment, peaks corresponding to carbon in sp^2 - bonding (284.53eV), sp^3 - bonding (285.05eV) and shake-up (290.71 eV) could still be observed. However, it is cleared that the ratio of XPS peak intensity between the sp^2 and sp^3 carbon (I_{sp^2}/I_{sp^3}) decreased after the plasma treatment process. Furthermore, an additional peak at 286.18 eV could be fitted to the C1s feature (Figure S4c). This new peak was derived from carbon bonded to oxygen. In addition, an O1s feature which was unresolvable in the pristine sample emerged in the plasma treated sample (Figure 4c and d). Upon deconvoluting the O1s feature, three peaks at 530.50, 532.90 and 537.20 eV were observed. These peaks correspond to physisorbed molecular oxygen or carbonate, carboxyl or hydroxyl groups bonded to an aromatic structure and C-O groups respectively. The emergence of O1s features correspond to the change in the C1s peak observed and collaborate with the interpretation that oxygen functionalization occurred once the plasma-treated CNT arrays had been exposed to air. As a result of the plasma functionalization, the atomic percentage of oxygen increased from 1.2% to 7%. This demonstrates that the plasma treatment was indeed able to modulate the chemical environment of the CNT arrays.

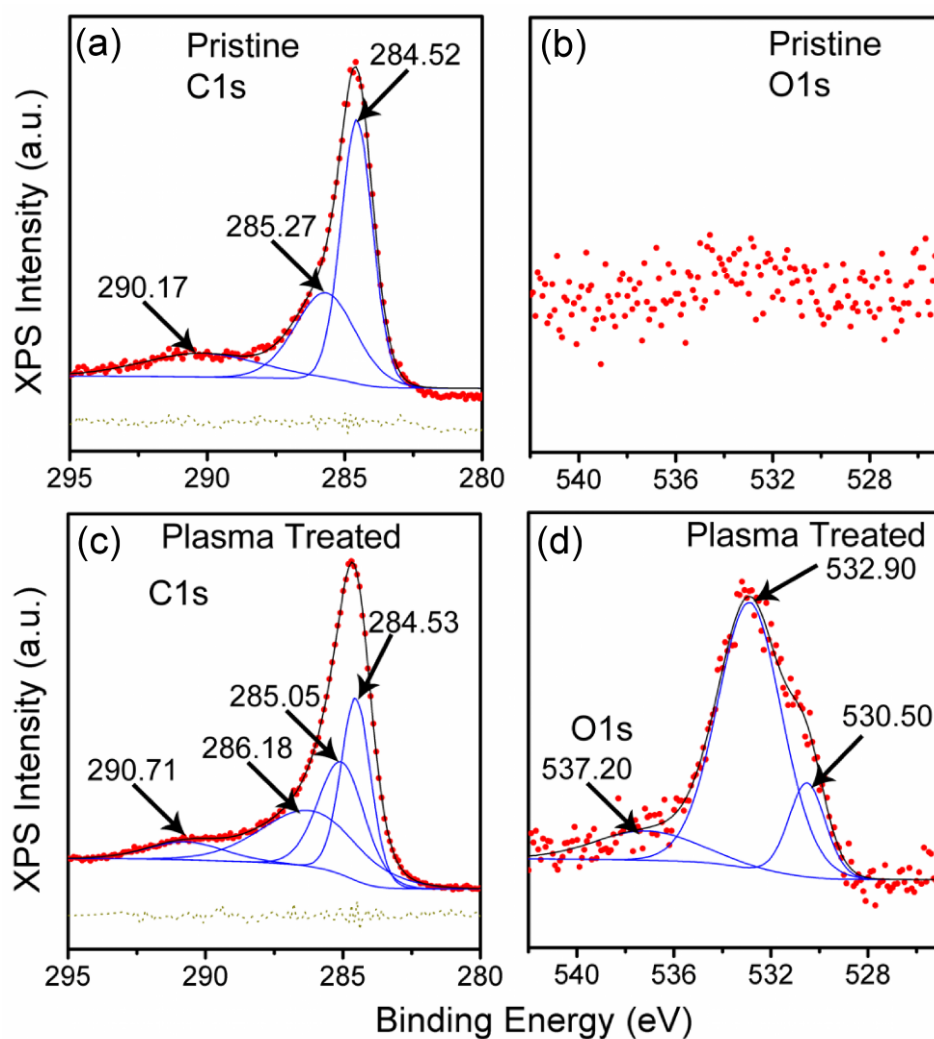


Fig. S4. XPS spectra of the pristine and 1000 W plasma treated CNT arrays with the binding energy of C1s (a), (c) and O1s (b),(d).

S6. Flow cytometry

Bacterial biofilms were scraped off the incubated CNTs into 2 ml phosphate buffered saline (PBS) using a sterile metal spatula. Samples were sonicated for 1 min before staining with LIVE/DEAD[®] BacLight[™] (Invitrogen) according to the manufacturer's instructions. A 6 h fresh culture of each strain was diluted into PBS. One half of this culture was used as a live control and stained with each of the components (SYTO 9 and PI) separately. The other half was heat killed by exposing the tube to 90 °C for 10 min in a water bath before staining and use as a dead control. Samples were run on a FACSCalibur flow cytometer (BD Biosciences, San Jose, USA), equipped with a 15 mW air-cooled 488 nm argon-ion laser. FACSFlow (BD Biosciences) was used as the sheath fluid. Green fluorescence (FL1-H) was collected through a 530 nm band-pass filter and red fluorescence (FL3-H) through a 650 nm long-pass filter. A minimum of 20000 events were collected on the basis of their forward-angle light scatter (FSC) and side scatter (SSC) properties. The instrument settings used throughout the experiments were FSC=E01, SSC=417 mV, FL1=602 mV, FL3=711 mV using logarithmic amplifiers. Samples were run at the low flow rate setting (12 μ L/s). Online data acquisition was with BD CellQuest Pro software (BD Biosciences) followed by offline analysis with FlowJo version 7.5.5 (TreeStar, Ashland, USA).

S7. The effects plasma treatment on CNT arrays have on *S. epidermidis* and *P. aeruginosa*

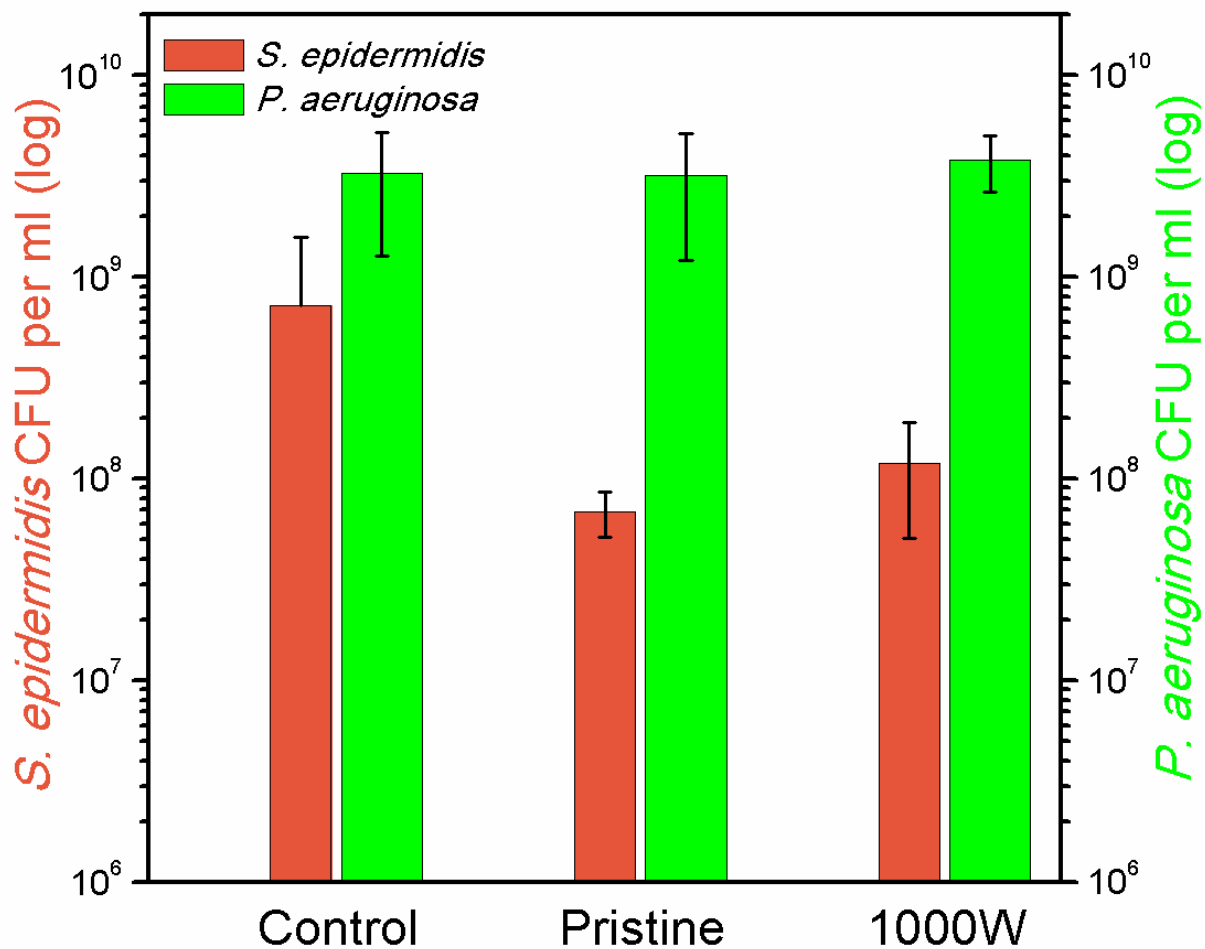


Fig. S5. Quantity of *S. epidermidis* and *P. Aeruginosa* on the control, pristine and plasma treated CNT arrays as shown by colony counting method.